Transported PDF Modelling and Analysis of Partially Premixed Flames

L. Tian, R. P. Lindstedt*

Department of Mechanical Engineering, Imperial College London, Exhibition Road, London SW7 2AZ, UK.

Abstract

A hybrid finite volume – transported joint probability density function (FV/JPDF) method is used to model piloted flames with inhomogeneous inlets. The flames were experimentally investigated using a retractable central tube within the main burner to control the degree of mixing at the exit. A five-gas (C_2H_2, H_2, CO_2, N_2, air) co–flow pilot located outside the burner was used to match the composition and adiabatic temperature of a stoichiometric methane/air flame. The applied hybrid method features a flow field calculation using a time-dependent finite-volume based method closed at the second-moment level with the scalar field obtained at the joint-scalar (JPDF) level. The current methodology is applicable to both premixed combustion and diffusion-dominated regions without assumption regarding the inclusion of the chemistry. Results show that the current method can accurately capture the stratified premixed flame mode near the burner exit as well as the diffusion-dominated flame far downstream. The transition between the combustion modes occurs around ten tube diameters downstream of the burner exit and it is observed that the flame structure is very sensitive to the prediction of the flow field in this region.

1. Introduction

Partially premixed flames caused by compositional inhomogeneities are common in practical combustion devices. Examples include flames in gas turbines, gas direct injection engines and industrial burners [1–3]. The intrinsic nature of multi-mode combustion presents difficulties for the application of regime dependent approaches such as the laminar flamelet concept [4] and conditional moment closures [5]. The transported PDF method has the potential to resolve such problems as the chemical reaction source term appears in closed form [6].

An excellent experimental database of partially premixed CH_4-air flames has been made available through the Sydney piloted burner with inhomogeneous inlets [7, 8]. The geometry features a concentric retractable inner tube that controls the degree of mixing at the burner exit plane. Subsequent measurements of temperature and species concentrations have been made at Sandia [8] and can be used to analyse the physics behind the transition from stratified-premixed to diffusion-dominated combustion. Attempts to develop rather simple combustion models have been made [9, 10] with significant deficiencies for highly inhomogeneous cases.

The current study considers a strongly inhomogeneous Sydney–Sandia case with a complex transition between combustion modes. The inner tube with pure methane was recessed into the outer air-supply tube by 75 mm (10 $\times$ the main tube diameter D_j). A five-gas (C_2H_2, H_2, CO_2, N_2, air) pilot was located outside the central burner assembly with the composition and adiabatic temperature matching that of a stoichiometric methane/air flame. A joint-scalar transported PDF method with the velocity field closed at the second moment level [11] is combined with a systematically reduced H/C/N/O mechanism featuring 300 reactions, 20 solved and 28 steady-state species for the thermochemistry and the modified Curl's model [12]. Computational results are compared with measurements along the radial direction at different axial positions.

2. Computational Model

The methodology used in the present study is based on a hybrid finite volume/joint transported PDF (FV/JPDF) method [11] with an extensively validated reduced H/C/N/O chemical mechanism [11, 13]. The flow field is solved using an elliptic time-dependent, two-dimensional axi-symmetric compressible flow solver closed at the second-moment level. The generalised Langevin model of Haworth and Pope [14] is used for the pressure redistribution terms and combined with a standard closure for the turbulent kinetic energy dissipation rate ($\widetilde{\epsilon}$) [15] with $C_{\epsilon 2}$ = 1.80. The JPDF method provides the scalar field and the density for the finite-volume part. The joint-scalar PDF is given below [6]:

$$\begin{aligned}\frac{\partial \bar{\rho}\widetilde{P}(\Psi)}{\partial t} + \frac{\partial \bar{\rho}\widetilde{u_l}\widetilde{P}(\Psi)}{\partial x_l} + \sum_{\alpha=1}^{N}\frac{\partial}{\partial \Psi_\alpha}(\bar{\rho}S_\alpha(\Psi)\widetilde{P}(\Psi)) \\ = -\frac{\partial}{\partial x_l}(\bar{\rho}\langle u_l''|\phi=\Psi\rangle\widetilde{P}(\Psi)) \\ + \sum_{\alpha=1}^{N}\frac{\partial}{\partial \Psi_\alpha}\left(\left\langle \frac{1}{\rho}\frac{\partial J_{l,\alpha}}{\partial x_l}\middle|\phi=\Psi\right\rangle\right) \end{aligned} \quad (1)$$

The above composition (and enthalpy) PDF equation is solved using a Monte–Carlo method featuring Lagrangian particles. The turbulent transport of the joint PDF is closed through a gradient diffusion approximation with the turbulent Prandtl number set to 0.7 and the mixing term is modelled using the modified Curl's model [12] using the standard scalar time-scale [11, 16] ratio defined in Eq. (2) with $C_\phi = 2.3$ [11, 13].

$$\tau_\phi^{-1} = \frac{\widetilde{\epsilon_\phi}}{\widetilde{\phi''^2}} = \frac{C_\phi}{2}\frac{\widetilde{\epsilon}}{\widetilde{k}} \quad (2)$$

3. Case Configuration

3.1 Experimental setup

The case (FJ200-5GP-Lr75-80) discussed below was investigated experimentally by Barlow et al. [8] using the configuration shown in Fig. 1. For the current study, the four concentric streams are, starting from the centreline, pure methane, air, pilot and co-flow air. Following the same order, the diameters of three tubes are 4, 7.5 and 18 mm, where $D_j = 7.5$ mm is defined as the main tube/burner diameter. The volumetric flow rate of the methane to air jets (V_F/V_A) is 1:2 with the fuel jet is recessed by $L_r = 75$ mm. Hence, the composition distribution varies along the burner exit. The average velocity at the burner exit was 80 m/s. The pilot has an unburnt bulk velocity

* Corresponding author: p.lindstedt@imperial.ac.uk

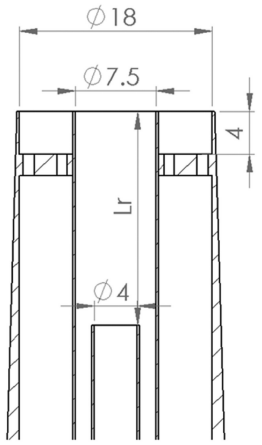

Figure 1: Schematic of the burner with dimensions in mm [8].

of 3.72 m/s (burnt velocity $\sim$ 24.14 m/s) and matches the C/H ratio and adiabatic temperature of a stoichiometric methane/air flame. Co-flow air is provided at a velocity of 15 m/s.

3.2 Computational setup

The present study is focussed on the turbulence-chemistry interactions above the burner exit. Hence, a 300 mm (axial) $\times$ 113 mm radial computational domain was used starting from the burner exit plane. The domains was discretised using 283 (axial) $\times$ 144 (radial) control volumes with a near burner resolution of 0.15 mm (radial) and 0.5 mm (axial).

The boundary conditions for the velocity field at the burner exit (current inflow) were obtained from the Large Eddy Simulation (LES) database shared by Mueller et al. [17]. Mean and fluctuating velocities of the co-flow follow the measurements [7] using the the same setup although with slightly different burner exit velocities. The mean velocity of the pilot was set to 24.1 m/s with a boundary layer of 1 mm thickness included for the shear layers. The fluctuating velocity was estimated using a linear interpolation between the main tube jet and the co-flow. The integral length scale was prescribed as $1/8^{th}$ of the main tube diameter, 0.07 of the hydraulic diameter in the pilot and from $L = \kappa y$ in the co-flow ($\kappa = 0.41$ is the von Karman constant and y is the perpendicular distance from the pilot surface). The dissipation rate was approximated by,

$$\widetilde{\epsilon} = \sqrt{\frac{3}{2}}(\frac{\widetilde{k}^{2/3}}{L}) \tag{3}$$

A transmissive boundary condition was for the perpendicular velocity at the outlet of the domain ($x = 300$ mm) with the remaining variables assigned using a von Neumann condition. A symmetric boundary was used at $r = 0$ mm. The profile of mixture fraction along the burner exit was also obtained from the LES database [17]. Approximately 120 stochastic particles were used each cell in the transported PDF method [11, 13].

The PDF calculation was initiated from a flamelet solution where the initial transients had vanished. It is noted that premixed unreacted mixtures is present and the use of a conventional $\beta-$ PDF based diffusion flame approach tends to overestimate the temperature in the burner region. As shown in Fig. 2a, measurements [8] also confirm that the fuel jet is not ignited. It was also observed in the present study that an erroneous estimation of the burner temperature obtained using flamelet data cannot be washed away by the transported PDF

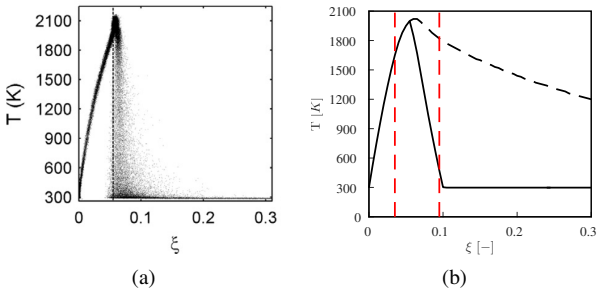

(a) (b)

Figure 2: Instantaneous scatter data for temperature against mixture fraction at $x/D_j = 1$ (a) [8] and a schematic of "cut-off" applied to the flamelet simulation (b). The nominal flammability limits of $0.035 \leq \xi \geq 0.095$ are indicated via the red dashed lines.

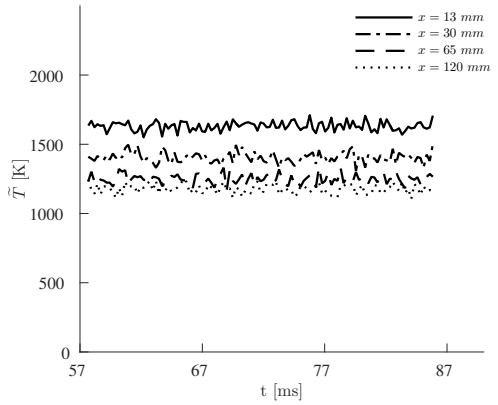

Figure 3: History of temperature at different axial locations, at radial position $r = 4$ mm. Lines as legends.

method. Hence, as illustrated in Fig. 2b, a gradual "cut-off" criterion between the stoichiometric value and the rich flammability limit was used to generate the flamelet look-up table.

4. Results

The case studied (FJ200-5GP-Lr75-80) was extensively discussed at the 13^{th} TNF workshop [18]. It is noted in the proceedings [18] that most of simulations fail to capture the mixing between fuel and air, leading to large discrepancies downstream the burner exit. Hence, radial profiles of mixture fraction and species are presented at four different axial locations downstream of the burner exit. As illustrated in Fig. 3, the current computations suggest that the flame burns stably and time averages of statistics between 58 ms and 85 ms are presented in Figs. 4 and 5.

4.1 Computed and measured mean scalar data

Figure 4a shows a comparison of the current predictions and measurement of the mean mixture fraction. It can be observed that the transported PDF method provides good agreement along the radial direction at different axial positions except for a slight discrepancy close to the centreline at $x/D_j = 15$. However, small discrepancies can have a significant impact on the flame structure. As shown in Fig. 4b, the predicted temperature agrees well with the measurement with the exception of $x/D_j = 15$. The over-estimation of mixture fraction close to

the centreline at $x/D_j = 15$ contributes to the slight under-prediction of temperature at the same location, whereas, the slight over-estimation of mixture fraction on the lean side leads to a substantial over-prediction of temperature. It is noted that the mixture fraction on the lean side is close to the lean flammability limit and hence a slight flow field discrepancy induces a much more significant difference in temperature due to ignition. It is also important to note that the flame undergoes a transition of combustion modes around $x/D_j = 15$. Overall, the premixed and diffusion flame modes are well captured with the dynamics of the transition between the two modes exceptionally sensitive to minor discrepancies in the flow field.

The production rate of CO is also very sensitive to the combustion regime. A very large scatter in results can be observed for CO among different groups/methods presented at the TNF workshop [18]. Radial profiles of CO obtained in the current study are shown in Fig. 4c. It can be observed the predictions agree well with experimental data at all axial locations although differences in the flow field leads to a modest over-prediction of CO at $x/D_j = 15$. Overall, Fig. 4c suggests that the current closure of the thermochemistry adequately represents the species concentrations for the different combustion modes.

4.2 Computed and measured scalar variances

Radial profiles of the mixture fraction variance are shown in Fig. 5a. The values are under-estimated at the burner exit but accurately picks up the location of two peaks. The agreement close to the centreline recovers further downstream. Hence, the under-estimation of fluctuating mixture fraction are likely influenced by the boundary conditions, especially the prescribed length scale. The predicted temperature variance is compared to the experiment in Fig. 5b. The transported PDF result captures the two-peak characteristic of temperature variance close to the burner exit and also the "jet-like" distribution at $x/D_j = 30$. Similarly to the profiles of mean temperature, the discrepancy at $x/D_j = 15$ is attributed to the reproduction of the flow field during the combustion mode transition (e.g. early ignition). Radial profiles of CO variance are shown in Fig. 5c. The predictions agrees well with the experiment at all axial locations.

5. Conclusions

The present study has explored the behaviour of Sydney/Sandia piloted flames with inhomogeneous jets using a hybrid FV/JPDF method. The PDF method was initialised by flamelet results based on a gradual "cut-off" criterion with boundary conditions at the burner exit obtained from a LES database. Results suggest that the applied thermochemistry combined with the transported PDF method can capture features of both stratified-premixed combustion close to the burner exit and diffusion-dominated combustion far downstream. However, it is also noted that the dynamics of the transition between the different combustion modes is exceptionally sensitive to flow field predictions and, potentially, to boundary conditions. It is hence suggested that further experimental and computational studies would be fully justified for this very interesting case.

Acknowledgements

Authors gratefully acknowledge the sharing of the LES database by Bruce Perry and Michael Mueller from Princeton University. Lu Tian would like to acknowledge the financial support of Imperial College PhD Scholarship.

References

[1] G. Staffelbach, L. Gicquel, G. Boudier, T. Poinsot, Proceedings of the Combustion Institute 32 (2009) 2909–2916.

[2] M.C. Drake, D.C. Haworth, Proceedings of the Combustion Institute 31 (2007) 99–124.

[3] N. Syred, J.M. Ber, Combustion and Flame 23 (1974) 143–201.

[4] N. Peters, Progress in Energy and Combustion Science 10 (1984) 319–339.

[5] A.Y. Klimenko, R.W. Bilger, Progress in energy and combustion science 25 (1999) 595–687.

[6] S.B. Pope, Physics of Fluids 24 (1981) 588–596.

[7] S. Meares, V.N. Prasad, G. Magnotti, R.S. Barlow, A.R. Masri, Proceedings of the Combustion Institute 35 (2015) 1477–1484.

[8] R.S. Barlow, S. Meares, G. Magnotti, H. Cutcher, A.R. Masri, Combustion and Flame 162 (2015) 3516–3540.

[9] S. Galindo, F. Salehi, M. Cleary, A. Masri, Proceedings of the Combustion Institute 36 (2017) 1759–1766.

[10] H. Wu, M. Ihme, Fuel 186 (2016) 853–863.

[11] T.S. Kuan, R.P. Lindstedt, Proceedings of the Combustion Institute 30 (2005) 767–774.

[12] J. Janicka, W. Kolbe, W. Kollmann, Journal of Non-Equilibrium Thermodynamics 4 (1979) 47–66.

[13] K. Gkagkas, R.P. Lindstedt, T.S. Kuan, Flow, Turbulence and Combustion 82 (2009) 493–509.

[14] D.C. Haworth, S.B. Pope, Physics of Fluids 29 (1986) 387–405.

[15] W.P. Jones, B.E. Launder, International Journal of Heat and Mass Transfer 15 (1972) 301–314.

[16] R.P. Lindstedt, E.M. Váos, Combustion and Flame 145 (2006) 495–511.

[17] B.A. Perry, M.E. Mueller, A.R. Masri, Proceedings of the Combustion Institute 36 (2017) 1767–1775.

[18] Proceedings of the TNF13 Workshop, Thirteenth International Workshop on Measurement and Computation of Turbulent Flames, Seoul, Korea, 7.28-7.30, 2016. http://www.sandia.gov/TNF/13thWorkshop/TNF13.html.

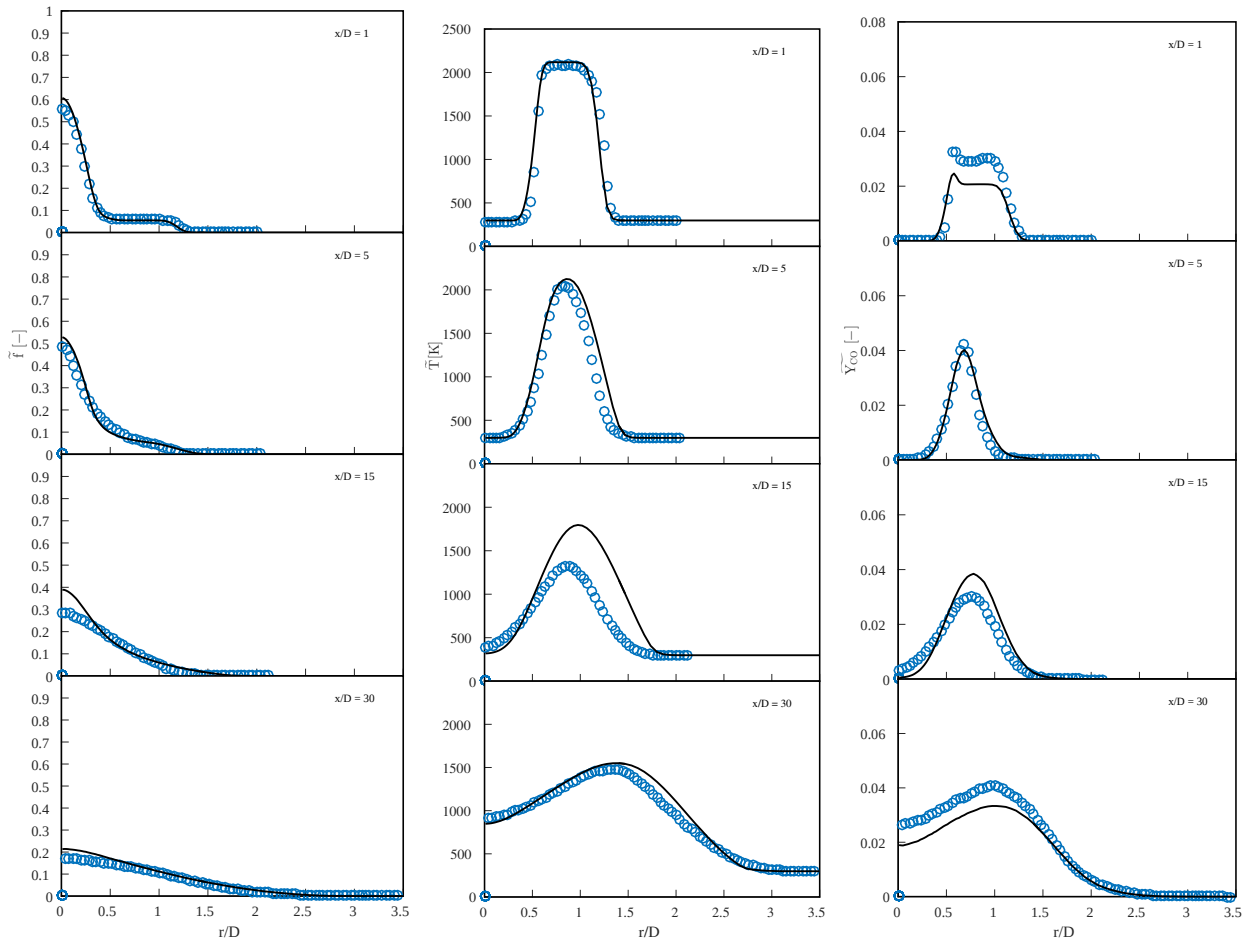

Figure 4: Radial profiles of mean mixture fraction (a), temperature (b) and CO mass fraction (c). Symbols and lines: (○) Experiment; (——) Transported PDF method.

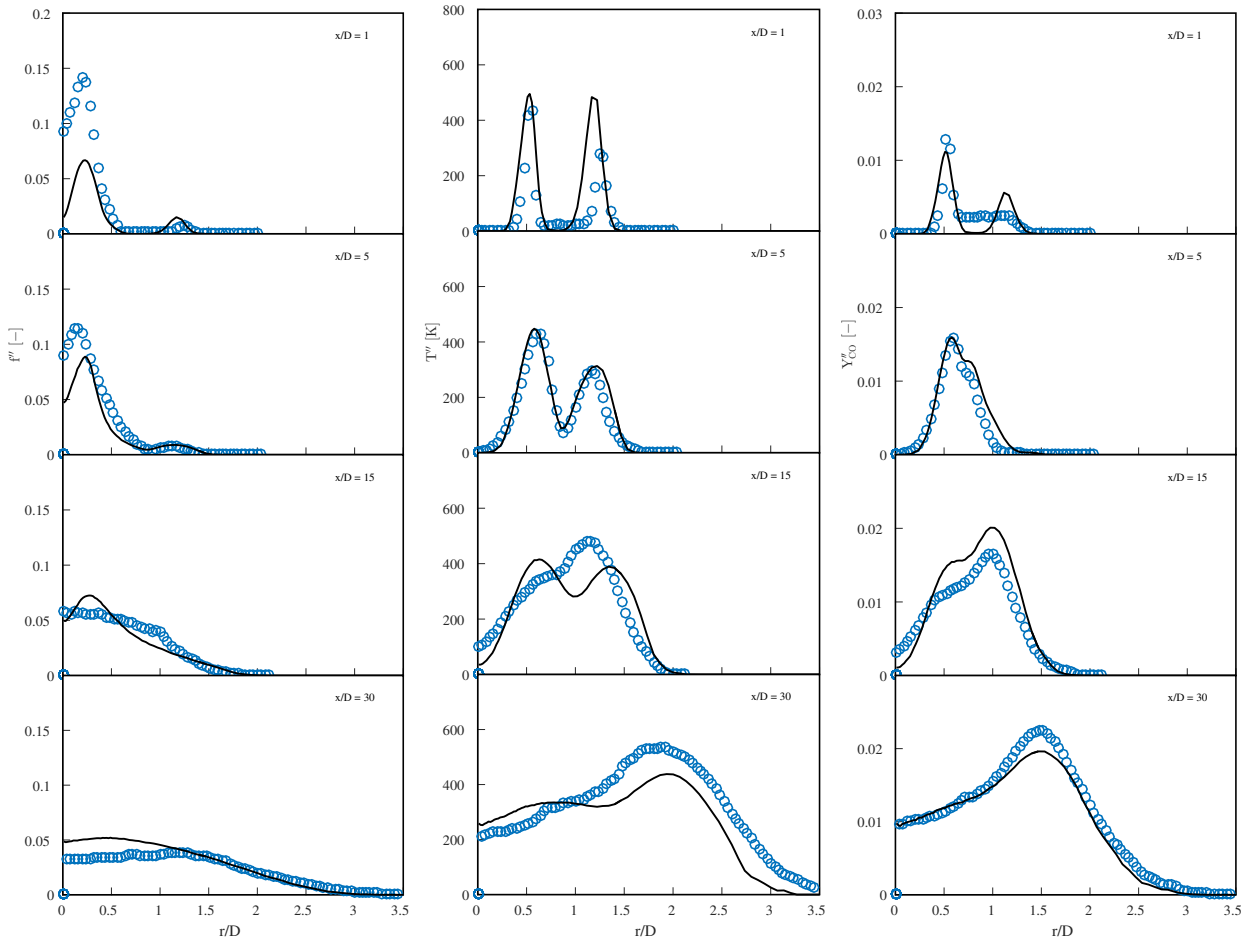

Figure 5: Radial profiles of fluctuating mixture fraction (a), temperature (b) and CO mass fraction (c). Symbols and lines: (○) Experiment; (——) Transported PDF method.